

IAN S: INTELLIGIBILITY-AWARE NULL-STEERING BEAMFORMING FOR DUAL-MICROPHONE ARRAYS

Wen-Yuan Ting^{*}, Syu-Siang Wang[†], Yu Tsao[‡], and Borching Su^{*}

^{*} Graduate Institute of Communication Engineering, National Taiwan University, Taipei, Taiwan

[†] Department of Electrical Engineering, Yuan Ze University, Taoyuan, Taiwan

[‡] Research Center for Information Technology Innovation, Academia Sinica, Taipei, Taiwan

ABSTRACT

Beamforming techniques are popular in speech-related applications due to their effective spatial filtering capabilities. Nonetheless, conventional beamforming techniques generally depend heavily on either the target's direction-of-arrival (DOA), relative transfer function (RTF) or covariance matrix. This paper presents a new approach, the intelligibility-aware null-steering (IAN S) beamforming framework, which uses the STOI-Net intelligibility prediction model to improve speech intelligibility without prior knowledge of the speech signal parameters mentioned earlier. The IAN S framework combines a null-steering beamformer (NSBF) to generate a set of beamformed outputs, and STOI-Net, to determine the optimal result. Experimental results indicate that IAN S can produce intelligibility-enhanced signals using a small dual-microphone array. The results are comparable to those obtained by null-steering beamformers with given knowledge of DOAs.

Index Terms— STOI, STOI-Net, null-steering, beamforming, microphone arrays

1. INTRODUCTION

Microphone arrays are commonly used in numerous speech-related applications including hearing aids and teleconferencing to isolate the desired signals that are often degraded by ambient noise and other types of interference [1, 2]. Multi-channel speech enhancement (MCSE) techniques have been extensively studied to extract the desired signals [3]. Beamforming algorithms are usually a crucial component of these methods, as they utilize spatial diversity from multiple recordings to perform spectral and spatial filtering on multiple channel inputs, generating a speech-enhanced output [4, 5]. For example, the delay-and-sum beamformer [6, Chapter 3] uses the geometry of the array and direction-of-arrival (DOA) information to parameterize the spatial-spectral filter. The minimum variance distortionless response (MVDR) method [7] minimizes the power of the noise signal while maintaining a distortionless response for the target signal, utilizing the knowledge of the covariance matrices and DOA or relative transfer function (RTF). Additionally, null-steering beamformers (NSBF) have been proposed to filter out signals from specific directions [8, 9, 10].

Conventional beamforming algorithms typically depend highly on an accurate DOA or RTF estimate to obtain the spatial information of the target signals. Over the past few decades, multiple DOA estimation algorithms have been proposed in [11, 12, 13]. For DOA estimation algorithms specialized for multiple speech signals, the work in [13] used the coherence test and sparsity property of speech

to estimate accurate DOAs using clustering-based methods. In addition to a direct DOA estimation approach, time difference of arrival (TDOA) estimation methods [14, 15, 16] are also commonly used to localize the target signal. One popular category is the application of the steered response power phase transform [14], which scans over a predefined spatial region to parameterize the cross-correlation functions using each candidate location of the source, and then adopts a maximum likelihood estimator to estimate the TDOA. In addition to these methods, the work in [17] discussed covariance subtraction and covariance whitening methods to obtain RTF estimates of the speech signal using well-estimated covariance matrices from noise-only and speech-noise frames. Although these approaches have great potential to provide accurate spatial information, they typically rely heavily on multiple assumptions. In the case of [17], the authors assumed accurate estimates of the noise covariance matrices for each time-frequency index. If the noise covariance matrices contain spatial statistics of the speech signal, the beamformers might not be aware of such errors and attenuate the corresponding signals without regard to how this might impact the intelligibility of speech signals. Meanwhile, it is also worth noting that, neural beamformers, such as [3, 18, 19, 20], have been proposed to perform state-of-the-art MCSE. For these NN-based approaches, it is usually necessary to construct a dataset containing diverse utterances received by a microphone array in multiple scenarios. In addition, these neural beamformers are usually optimized over a large number of parameters, which makes each parameter hard to interpret.

In the field of speech processing, a well-known metric for intelligibility is the short-time objective intelligibility (STOI) [21]. The STOI function estimates the intelligibility of signals through a series of signal-processing stages, including silence-segment elimination, feature extraction in the time-frequency (TF) domain, one-third octave band processing, feature normalization, and intelligibility mapping. In this process, the deteriorated sound signal and the corresponding clean reference signal are used simultaneously to compute the final score. In this paper, the STOI function will be denoted as $h_{\text{STOI}} : \mathbb{R}^{N \times K} \times \mathbb{R}^{N \times K} \rightarrow [0, 1]$ which is defined as the mapping from the magnitude of a pair of $N \times K$ short-time Fourier transform (STFT) matrices to the interval $[0, 1]$, where N is the number of time frames and K is the number of frequency bins per frame. For simplicity, we will omit the steps such as silence-segment elimination for our description of the STOI function. In addition, unlike metrics such as the speech intelligibility index in [22], STOI is known for its reliable intelligibility evaluation of signals processed in the TF domain, where most acoustic beamforming systems perform MCSE. However, a clean reference is typically inaccessible. Therefore, the authors in [23] proposed STOI-Net, a non-intrusive intelligibility as-

assessment model that predicts STOI scores based only on the noise-corrupted waveforms.

In light of the heavy dependence of beamformers on the estimation of the DOAs or RTFs of the speech signals, we propose a new optimization framework for an intelligibility-enhancing beamformer without relying on the previously mentioned speech parameters. Instead, we explicitly consider intelligibility as an optimization objective. Works such as [24] have also incorporated the notion of intelligibility into the design of beamformers. We will perform intelligibility-based optimization within a set of null-steering beamformers. Hence, we call this intelligibility-aware null-steering (IANS) beamforming. For the IANS beamforming process, an NSBF algorithm is first applied to generate a set of candidate signals via null-steering. The generated signals are then passed through a pre-trained STOI-Net to predict the associated STOI scores. IANS then outputs the utterance corresponding to the highest intelligibility score. Contrary to the previously mentioned neural beamformers, the proposed IANS algorithm doesn't require additional multi-channel training data. Moreover, the IANS optimization problem only optimizes one parameter whose optimal value is interpretable. Furthermore, advanced single-channel SE methods, such as [25, 26, 27, 28, 29], can be incorporated with IANS for downstream applications.

The remainder of this paper is organized as follows. Section 2 discusses the signal model and related works including filter-and-sum beamformers, null-steering beamformers and STOI-Net. Next, we will present our IANS optimization problem in Section 3. In Section 4, the IANS algorithm will be discussed in detail. Section 5 presents the experimental setup and results. Finally, Section 6 concludes the paper and discusses future works.

2. BACKGROUND AND RELATED WORKS

2.1. Signal model

In this study, the considered signal model comprises a speech signal, $s(t)$, and an interference signal, $i(t)$, propagating in a room with a sound speed of c , received by a dual-microphone array at angles of θ_s and θ_i , respectively. The angles are measured with respect to the first (reference) microphone, with 0° being the endfire direction. The microphone array has a small spacing of ℓ , and we assume that the sound sources are stationary in space. We denote the room impulse responses (RIRs) for $s(t)$ and $i(t)$ with respect to the m^{th} microphone as $g_s^{(m)}(t)$ and $g_i^{(m)}(t)$, respectively. The received signal at the m^{th} microphone can be expressed as the following:

$$x^{(m)}(t) = g_s^{(m)}(t) * s(t) + g_i^{(m)}(t) * i(t). \quad (1)$$

After obtaining the received signals $x^{(1)}(t)$ and $x^{(2)}(t)$, We can then apply the STFT to derive their corresponding $N \times K$ STFT matrices $\mathbf{X}^{(1)}$ and $\mathbf{X}^{(2)}$. Subsequently, we can define the received signal vector $\mathbf{x}[n, k]$ as follows:

$$\mathbf{x}[n, k] = [\mathbf{X}_{n,k}^{(1)}, \mathbf{X}_{n,k}^{(2)}]^T. \quad (2)$$

Here, $\mathbf{X}_{n,k}^{(m)}$ represents the $(n, k)^{\text{th}}$ element of $\mathbf{X}^{(m)}$, where $n = 1, 2, \dots, N$ and $k = 1, 2, \dots, K$.

2.2. Filter-and-sum beamformers

Filter-and-sum beamformers [30] are a set of beamformers that perform the filter-and-sum operation to enhance the signal of interest. This process can be represented in the TF-domain as

$$Y[n, k] = \mathbf{w}^H[n, k] \mathbf{x}[n, k], \quad (3)$$

where $\mathbf{w}[n, k]$ is the weight vector for $\mathbf{x}[n, k]$, and $Y[n, k]$ is the resulting TF component of the beamformed signal. We will denote this set of beamformers as $\mathcal{F}_{\text{FSBF}}$.

2.3. Null-steering beamformers

Within $\mathcal{F}_{\text{FSBF}}$, there is a subset of beamformers capable of nulling out signals coming from a particular direction ϕ while maintaining a (nearly) distortionless response at θ_d . We call this set the null-steering beamformer set, $\mathcal{F}_{\text{NSBF}}$.

We first define two vectors, the distortionless response steering vector $\mathbf{a}^{(\theta_d)}[k] = [1, e^{-j\frac{\omega_k \ell}{c} \cos \theta_d}]^T$ and the null-response steering vector $\mathbf{a}^{(\phi)}[k] = [1, e^{-j\frac{\omega_k \ell}{c} \cos \phi}]^T$, where ω_k is the frequency value at the k^{th} frequency bin. Each $\mathbf{a}^{(\phi)}[k]$ is associated with a projection matrix $\Phi[k]$ defined in the following,

$$\begin{aligned} \Phi[k] &= \mathbf{I} - \frac{\mathbf{a}^{(\phi)}[k] (\mathbf{a}^{(\phi)}[k])^H}{\|\mathbf{a}^{(\phi)}[k]\|^2} \\ &= \mathbf{I} - \frac{\mathbf{a}^{(\phi)}[k] (\mathbf{a}^{(\phi)}[k])^H}{2}, \end{aligned} \quad (4)$$

where $(\cdot)^H$ denotes the Hermitian transpose operator. Here, $\Phi[k]$ projects vectors into the subspace orthogonal to the span of $\mathbf{a}^{(\phi)}[k]$. In this paper, $\mathcal{F}_{\text{NSBF}}$ is defined as a beamformer set with time-invariant weight vectors defined as

$$\mathbf{w}[k] = \frac{\Phi[k] \mathbf{a}^{(\theta_d)}[k]}{\max((\mathbf{a}^{(\theta_d)}[k])^H \Phi[k] \mathbf{a}^{(\theta_d)}[k], \epsilon)}, \quad (5)$$

where ϵ is a small number to avoid 0 division. We note that without the $\max(\cdot, \epsilon)$, Eq. (5) has been studied in [31] in the context of the MVDR beamformer. It is also worth pointing out that in the context of beamformers such as the linearly-constrained minimum variance beamformer [30], null responses are usually set as explicit constraints to a noise power minimization problem.

2.4. STOI-Net

In [23], the authors proposed STOI-Net, a non-intrusive speech intelligibility assessment model that predicts the STOI scores of speech signals both frame- and utterance-wise using feature extraction and score calculation functions. For the feature extraction, the STFT is applied to convert the peak-normalized time-domain waveform of interest into a sequence of frame-wise magnitude spectra in the frequency domain. These frames are then passed through 12 fully convolutional neural network layers to extract the acoustic representations. Next, the score-calculation function maps the extracted features to an intelligibility score. Specifically, frame-level scores are generated after applying 1) bidirectional long short-term memory, 2) an attention layer, and 3) fully connected nonlinear mapping functions to the extracted features. The final intelligibility score of the entire utterance is then obtained by applying a global averaging algorithm to all frame-level scores. It is worth noting that STOI-Net is not limited to a single neural network architecture. In [23], two model architectures were used: one with an attention layer and the other without it. In the remainder of this paper, we will denote the STOI-Net model as a function $h_{\text{STOI-Net}} : \mathbb{R}^{N \times K} \rightarrow \mathbb{R}$.

3. PROBLEM FORMULATION

Contrary to most optimal beamformers for speech enhancement (e.g., MVDR) where optimal weights are derived for each TF bin based on well-estimated DOAs, RTFs and covariance matrices, we

propose an optimization problem based on the intelligibility of the entire utterance of the received speech signals.

Our primary goal is to identify a function $f : \mathbb{C}^{N \times K} \times \mathbb{C}^{N \times K} \rightarrow \mathbb{C}^{N \times K}$ within a function set \mathcal{F} that takes the received signals $\mathbf{X}^{(1)}$ and $\mathbf{X}^{(2)}$ as input and maps them to an STFT matrix with the maximum STOI score. As we aim to perform optimization without having to train a new NN that learns from a dataset containing microphone array recordings from various scenarios, we will use a simpler function set $\mathcal{F} = \mathcal{F}_{\text{NSBF}}$ where we can limit all potential values of θ_d and ϕ on a discrete grid. However, the number of feasible solutions grows quadratically with the resolution for the θ_d and ϕ axes on this grid. Hence, we only perform grid search for ϕ on a grid \mathcal{G} while fixing θ_d to an arbitrary angle $\psi \in [0^\circ, 180^\circ]$. The grid \mathcal{G} is an ordered set containing P angles ranging from 0° to 180° . Thus, the number of possible beamformers we are considering here is P . Our optimization problem can now be described as the following:

$$\begin{aligned} & \underset{\phi \in \mathcal{G}}{\text{maximize}} && h_{\text{STOI}}(|f_{\theta_d=\psi, \phi}(\mathbf{X}^{(1)}, \mathbf{X}^{(2)})|, |\mathbf{S}|) \\ & \text{subject to} && f_{\theta_d=\psi, \phi} \in \mathcal{F}_{\text{NSBF}}, \end{aligned} \quad (6)$$

where \mathbf{S} represents the STFT matrix of the clean speech signal and $|\cdot|$ denotes the element-wise magnitude extraction for a matrix. We refer to this problem as the STOI Null-steering (STOI-NS) problem, as it employs null-steering to optimize the true STOI function. We will denote the optimal beamformer and null angle for this problem as $f_{\text{STOI-NS}}^*$ and $\phi_{\text{STOI-NS}}^*$, respectively.

However, \mathbf{S} is never accessible in practical scenarios. Therefore, using the pre-trained STOI-Net model $h_{\text{STOI-Net}}$, we modify the optimization problem in (6) as follows:

$$\begin{aligned} & \underset{\phi \in \mathcal{G}}{\text{maximize}} && h_{\text{STOI-Net}}(|f_{\theta_d=\psi, \phi}(\mathbf{X}^{(1)}, \mathbf{X}^{(2)})|) \\ & \text{subject to} && f_{\theta_d=\psi, \phi} \in \mathcal{F}_{\text{NSBF}} \end{aligned} \quad (7)$$

Since STOI-Net was trained to estimate the STOI score of a signal, we consider this the Intelligibility-aware Null-steering (IANS) problem. The IANS problem is now feasible without the clean reference \mathbf{S} . The optimal beamformer and null angle for this problem are denoted as f_{IANS}^* and ϕ_{IANS}^* , respectively. It is clear that the STOI score of the output obtained from using the beamformer $f_{\text{STOI-NS}}^*$ is a natural upper bound of that using f_{IANS}^* as we will show in Section 5. This optimization framework was inspired by works such as [28], where the authors trained speech enhancement systems by incorporating speech quality prediction neural networks [32] into the loss function.

Notably, contrary to conventional beliefs where it is generally thought to be necessary for ψ to be close to θ_s in order to perform speech enhancement, our method as we will show later in Section 5 is no longer constrained to this requirement. Therefore, we do not regard ψ as an estimate of θ_s . This also implies that, in the context of the STOI-NS and IANS optimization problem, we never guarantee the distortionless property of speech as in the MVDR beamformer. However, as we will show later in Section 5, intelligibility enhancement is still possible using the optimal null angles $\phi_{\text{STOI-NS}}^*$ and ϕ_{IANS}^* . These two angles can be interpreted as optimal null angles chosen to minimize the impact of the interference signal, speech distortion and RIRs on intelligibility, while maintaining a nearly distortionless response at ψ . Since there is a chance that $\psi = \theta_i$, it is advisable to perform the IANS algorithm twice using two different θ_d values (e.g., ψ and $\psi + 80^\circ$ in this study).

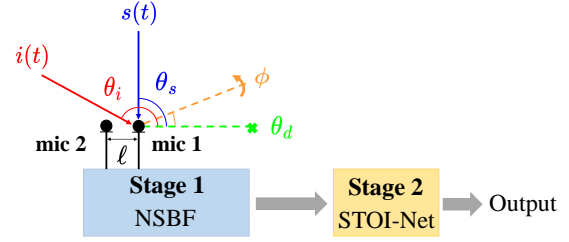


Fig. 1. IANS block diagram

It is worth noting that dual-microphone array beamformers usually correspond to beam patterns exhibiting a large main lobe and side lobe owing to the limited degrees of freedom. In other words, we can use this property to construct a directive null, as in Eq. (4), while preserving a certain amount of gain for signals coming from all angles, except those within the vicinity of the null. We also note that small microphone arrays tend to have frequency-invariant beam patterns as explained in [33], which can also be an advantage since beamformers that are sensitive to frequency variations tend to produce more unpredictable results.

4. THE IANS ALGORITHM

This section describes the IANS algorithm which solves the IANS optimization problem in (7). The algorithm consists of two stages: the NSBF stage and the STOI-Net stage as shown in Fig. 1, where results from the first stage will be passed on to the second stage. The following subsections will provide more detailed explanations about the IANS algorithm.

4.1. Stage 1: NSBF

The initial step of the IANS algorithm involves applying the STFT on the two signals $x^{(1)}(t)$ and $x^{(2)}(t)$ to obtain $\mathbf{X}^{(1)}$ and $\mathbf{X}^{(2)}$. We then generate a set $\mathcal{Y}_{(\text{STFT})}$ containing P STFT matrices $\{\mathbf{Y}^{(1)}, \dots, \mathbf{Y}^{(P)}\}$ by sending the pair $(\mathbf{X}^{(1)}, \mathbf{X}^{(2)})$ into P NSBF beamformers $\{f_{\theta_d=\psi, \phi=\mathcal{G}_1}, \dots, f_{\theta_d=\psi, \phi=\mathcal{G}_P}\} \subset \mathcal{F}_{\text{NSBF}}$. If $\psi = \mathcal{G}_p$, where $p \in \{1, 2, \dots, P\}$, we let $\mathbf{Y}^{(p)} = \mathbf{X}^{(1)}$ instead of using $f_{\theta_d=\psi, \phi=\psi}$. Note that parallel computing can be used since each computation of the elements of $\mathcal{Y}_{(\text{STFT})}$ is independent of each other. It is also worth pointing out that the time-invariant weight vectors in Eq. (5) can be computed and stored beforehand to save time.

Since we will later send these into STOI-Net, we apply the inverse-STFT operation (iSTFT) on each element in $\mathcal{Y}_{(\text{STFT})}$ to perform peak normalization in the time domain. We denote this set as $\mathcal{Y}'_{(\text{time})}$. We do this to match the training conditions of STOI-Net as we mentioned in Subsection 2.4.

4.2. Stage 2: STOI-Net

Following the peak normalization, we perform STFT on each element in $\mathcal{Y}'_{(\text{time})}$ to convert them back to the TF domain and extract their corresponding magnitude components. We denote the resulting set as $\mathcal{Y}''_{(\text{STFT})}$. We then pass each element in $\mathcal{Y}''_{(\text{STFT})}$ into STOI-Net to predict their utterance-based STOI score. These scores are then stored in a STOI-Net score vector α . The optimal null angle ϕ_{IANS}^* for f_{IANS}^* can be obtained as

$$\phi_{\text{IANS}}^* = \mathcal{G}_{\text{argmax}(\alpha)}. \quad (8)$$

Moreover, in the case where we have access to the clean reference signal \mathbf{S} , we can replace STOI-Net with the real STOI function in

this stage and obtain a STOI score vector β . Therefore, the value of $\phi_{\text{STOI-NS}}^*$ for $f_{\text{STOI-NS}}^*$ can be expressed as

$$\phi_{\text{STOI-NS}}^* = \mathcal{G}_{\text{argmax}(\beta)}. \quad (9)$$

In this study, the pre-trained STOI-Net model without the attention layer was directly obtained from the previous research¹ without any modifications, such as adaptation, retraining, or fine-tuning, for the MCSE task.

5. EXPERIMENTAL RESULTS AND ANALYSIS

5.1. Experimental setup

In this study, the Pyroomacoustics package [34] was utilized to simulate the signal model in Eq. (1) using the image source method [35] with the following parameters. The simulated room has dimensions of [5 m, 6 m, 4 m] with the RT60 parameter set to 150 ms and the sound speed c set to 343 m/s. The center of the microphone array is located at [2.5 m, 3 m, 1 m]. The distance between the two microphones is set to $\ell = 8$ mm with the array being parallel to the x-axis and the reference microphone being the microphone on the right. The speech DOA θ_s is set to 90° , while the interference DOA θ_i can be one of four predefined directions: 22.5° , 67.5° , 112.5° , or 157.5° . IANS then uses 512-point Hamming windows with 50% overlap to process the incoming signals. The set \mathcal{G} is a uniform grid over the interval $[0^\circ, 180^\circ]$ with an angular resolution of 2° (i.e., 91 angular values). Additionally, IANS was evaluated using two values for ψ : 0° , representing the largest angle difference from θ_s , and 80° , which is relatively closer to θ_s . Note that the values of ℓ and c are assumed known to the IANS algorithm. Additionally, the value of $\epsilon = 1.11 \times 10^{-16}$.

Our experiments can be classified into two parts. The first part uses an English dataset, namely, the Wall Street Journal [36] eval92 evaluation set. From eval92, we first selected two male and two female speakers, and chose one utterance from each speaker to form the source signal. Babble and car noises in the NOISEUS corpus [37, Chapter 12] and pink noise in NOISEX-92 [38] were applied as the interference. Five signal-to-interference ratios (SIRs), namely, -10 , -5 , 0 , 5 , and 10 dB, were used to create noisy utterances. The SIRs were mixed with respect to the first microphone as suggested by the Pyroomacoustics documentation. Therefore, 240 source-interference pairs (four clean utterances, three noises, four interference angles, and five SIRs) were used to form the English testing set (denoted as “WSJ”). For the second part of experiments, we used a Mandarin dataset, namely, the Taiwan Mandarin Hearing in Noise Test [39] corpus, comprising 320 sentences. Two male speakers and two female speakers were selected from the dataset. One utterance, recorded in a noise-free environment, was selected from each speaker as the speech source. For the interference signal, we chose three noise signals from the DEMAND [40] dataset: “metro”, “pstation”, and “npark.” Like in WSJ, the aforementioned SIRs were used to create 240 source-interference pairs (four clean utterances, three noises, four interference angles, and five SIRs) for the Mandarin testing set (denoted as “TMHINT”). It is worth noting that STOI-Net was previously trained on the training set of the original Wall Street Journal dataset. The eval92 set was used to evaluate the generalization performance of STOI-Net. Therefore, the English and Mandarin datasets in this study correspond to the matched and mismatched languages for STOI-Net, respectively. All single-channel recordings were sampled at 16 kHz. The experimental performance was evaluated in terms of STOI and the wideband extension of the perceptual evaluation of speech quality (PESQ) [41, 42] metric.

¹<https://github.com/dhimasryan/STOI-Net>

5.2. Evaluation results

For both testing sets, we labeled the enhanced results using the IANS algorithm with $\theta_d = \psi$ as “IANS $_\psi$.” Noisy utterances (labeled as “Noisy”) received by the first microphone were used as the baseline. Moreover, we also compared our IANS result with two additional systems. The first system is the STOI-NS system which optimizes the STOI-NS problem given the clean reference \mathbf{S} for all utterances. The optimization procedure was detailed in Section 4. Like in “IANS $_\psi$ ”, we represent the results from STOI-NS with $\theta_d = \psi$ as “STOI-NS $_\psi$.” For the second system, NSBF was performed by setting $\theta_d = \theta_s$ and $\phi = \theta_i$. This system has the advantage of knowing the true DOAs of the speech and interference signals. Therefore, we label the corresponding results as “T-NSBF.”

For the WSJ evaluation set, we list the average STOI and PESQ scores for all 240 utterances of “Noisy”, “IANS $_{0^\circ}$ ”, “STOI-NS $_{0^\circ}$ ”, and “T-NSBF” in Table 1. From the table, we can see that the STOI and PESQ scores for “IANS $_{0^\circ}$ ” are higher than those for “Noisy”, indicating an improvement in the intelligibility and quality of noisy speech signals from the English dataset using the proposed approach. Table 2 lists the STOI and PESQ scores of “Noisy”, “IANS $_{0^\circ}$ ”, “STOI-NS $_{0^\circ}$ ”, and “T-NSBF” associated with the TMHINT database. From the table, the improved metric performances from “Noisy” to “IANS $_{0^\circ}$ ” confirm that the proposed IANS method can effectively enhance the intelligibility and sound quality of noise-corrupted utterances. Notably, in both Tables 1 and 2, STOI-NS $_{0^\circ}$ has the highest STOI and PESQ scores on average, indicating that in these two experiments, if we properly choose the null angle to be $\phi_{\text{STOI-NS}}^*$, we generate results with even higher intelligibility and quality than the results from null-steering beamforming where we had the prior knowledge of the DOAs of the speech and interference signals. One potential factor that may have influenced this outcome is the non-anechoic nature of the room, resulting in signals propagating through multiple pathways. Hence, nulling the angle θ_i may not be the optimal choice for STOI.

Next, we will further investigate how different values of ψ af-

Table 1. Average STOI and PESQ scores for “Noisy”, “IANS $_{0^\circ}$ ”, “STOI-NS $_{0^\circ}$ ”, and “T-NSBF” on WSJ

	Noisy	IANS $_{0^\circ}$	STOI-NS $_{0^\circ}$	T-NSBF
STOI	0.765	0.857	0.862	0.858
PESQ	1.277	1.538	1.581	1.553

Table 2. Average STOI and PESQ scores for “Noisy”, “IANS $_{0^\circ}$ ”, “STOI-NS $_{0^\circ}$ ”, and “T-NSBF” on TMHINT

	Noisy	IANS $_{0^\circ}$	STOI-NS $_{0^\circ}$	T-NSBF
STOI	0.820	0.881	0.895	0.892
PESQ	1.417	1.614	1.770	1.744

Table 3. Average STOI and PESQ scores for “IANS $_{0^\circ}$ ”, “IANS $_{80^\circ}$ ”, “STOI-NS $_{0^\circ}$ ”, and “STOI-NS $_{80^\circ}$ ” on WSJ

	IANS $_{0^\circ}$	IANS $_{80^\circ}$	STOI-NS $_{0^\circ}$	STOI-NS $_{80^\circ}$
STOI	0.857	0.857	0.862	0.862
PESQ	1.538	1.541	1.581	1.583

Table 4. Average STOI and PESQ scores for “IANS $_{0^\circ}$ ”, “IANS $_{80^\circ}$ ”, “STOI-NS $_{0^\circ}$ ”, and “STOI-NS $_{80^\circ}$ ” on TMHINT

	IANS $_{0^\circ}$	IANS $_{80^\circ}$	STOI-NS $_{0^\circ}$	STOI-NS $_{80^\circ}$
STOI	0.881	0.881	0.895	0.895
PESQ	1.614	1.615	1.770	1.771

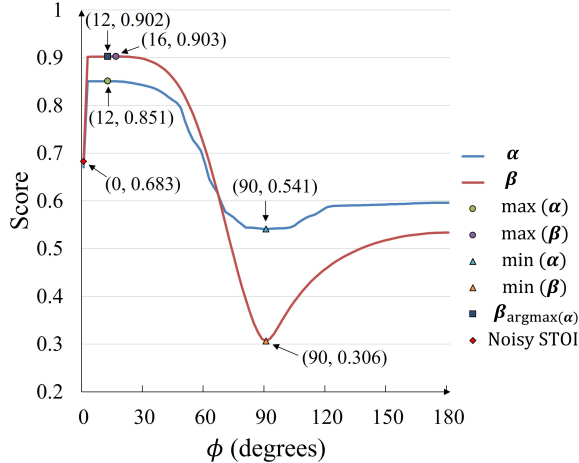


Fig. 2. Comparing the STOI-Net score vector α from IANS with STOI score vector β from STOI-NS in Scenario A using $\psi = 0^\circ$

fects the performance of “IANS $_\psi$ ” and “STOI-NS $_\psi$.” Specifically, we compared the results obtained using $\psi = 0^\circ$ and $\psi = 80^\circ$. These results are presented in Tables 3 and 4, which correspond to the WSJ and TMHINT databases, respectively. From both tables, when comparing “IANS $_{0^\circ}$ ” with “IANS $_{80^\circ}$ ” and “STOI-NS $_{80^\circ}$ ”, we can see that, even though the results corresponding to $\psi = 80^\circ$ yield higher PESQ scores, there is essentially no difference in STOI. This implies that the large 90° difference between ψ and θ_s has an insignificant effect on the ability of the IANS algorithm to generate intelligibility-enhanced results in our experiments.

Finally, we present an additional analysis of α and β in a particular scenario (Scenario A) to gain further insight into the similarities between the IANS and STOI-NS problems. The scenario consists of a female speaker from the WSJ dataset being interfered by the babble noise coming from a 22.5° angle (i.e., $\theta_i = 22.5^\circ$) with the SIR set to 0 dB. We let $\psi = 0^\circ$ for both IANS and STOI-NS, which means that the STOI value in β corresponding to $\phi = 0^\circ$ is the STOI score of the unprocessed signal at the reference microphone as we explained in Subsection 4.1. The score values in both α and β are represented by the two curves depicted in Fig. 2. The x-axis represents the values of ϕ in degrees, whereas the y-axis represents the values of α and β . From the figure, we can see that the two curves have similar characteristics. Specifically, the lowest values for α and β both correspond to $\phi = \theta_s = 90^\circ$. Since both f_{IANS}^* and $f_{\text{STOI-NS}}^*$ output results corresponding to the largest value in their respective score vectors, this suggests that they are both effective in preventing the speech signal from being severely attenuated in Scenario A. Moreover, maximum values of α and β occur at $\phi_{\text{IANS}}^* = 12^\circ$ and $\phi_{\text{STOI-NS}}^* = 16^\circ$, respectively. The corresponding STOI scores for f_{IANS}^* and $f_{\text{STOI-NS}}^*$ are 0.902 (i.e., $\beta_{\text{argmax}(\alpha)}$) and 0.903 (i.e., $\max(\beta)$), respectively, which are at least 0.219 points higher than the STOI score of “Noisy” at 0.683, indicating the effectiveness in STOI enhancement of our IANS algorithm.

6. CONCLUSION AND FUTURE WORK

In this paper, we proposed a novel intelligibility-based optimization problem (i.e., the IANS problem) along with its corresponding enhancement system, the IANS beamformer. The system determines the optimal output speech with the highest intelligibility scores by combining the NSBF and STOI-Net modules, where NSBF processes the input recordings and STOI-Net provides STOI predic-

tions. We conducted experiments using cross-lingual datasets (Mandarin and English). The experimental results show that the proposed IANS system can effectively map the input signals to intelligibility and quality enhanced speech. It was also demonstrated that IANS produces robust performance regardless of whether the distortionless response is steered near the direction of the speech source. In the future, we will evaluate the combination of beamforming systems with different evaluation modules, such as quality and mean opinion score assessment models [43], and test our system in more complex noisy environments. In addition, we will integrate single-channel speech enhancement methods with IANS to further enhance speech signals.

7. REFERENCES

- [1] R. Chakraborty and C. Nadeu, “Joint recognition and direction-of-arrival estimation of simultaneous meeting-room acoustic events,” in *Proc. INTERSPEECH*, 2013, pp. 2948–2952.
- [2] K. Kumatani, B. Raj, R. Singh, and J. McDonough, “Microphone array post-filter based on spatially-correlated noise measurements for distant speech recognition,” in *Proc. INTERSPEECH*, 2012, pp. 298–301.
- [3] T. Ochiai, S. Watanabe, T. Hori, J. R. Hershey, and X. Xiao, “Unified architecture for multichannel end-to-end speech recognition with neural beamforming,” *IEEE Journal of Selected Topics in Signal Processing*, vol. 11, no. 8, pp. 1274–1288, 2017.
- [4] H. Cox, R. Zeskind, and M. Owen, “Robust adaptive beamforming,” *IEEE Transactions on Acoustics, Speech, and Signal Processing*, vol. 35, no. 10, pp. 1365–1376, 1987.
- [5] X. Wang, I. Cohen, J. Benesty, and J. Chen, “Study of the null directions on the performance of differential beamformers,” in *Proc. ICASSP*, 2022, pp. 4928–4932.
- [6] M. R. Bai, J.-G. Ih, and J. Benesty, *Acoustic array systems: theory, implementation, and application*, John Wiley & Sons, 2013.
- [7] J. Capon, “High-resolution frequency-wavenumber spectrum analysis,” *Proceedings of the IEEE*, vol. 57, no. 8, pp. 1408–1418, 1969.
- [8] H. Schepker, L. T. T. Tran, S. Nordholm, and S. Doclo, “Acoustic feedback cancellation for a multi-microphone ear-piece based on a null-steering beamformer,” in *Proc. IWAENC*, 2016, pp. 1–5.
- [9] M. Z. Ikram and D. R. Morgan, “A beamforming approach to permutation alignment for multichannel frequency-domain blind speech separation,” in *Proc. ICASSP*, 2002, pp. 881–884.
- [10] C. Li, J. Benesty, and J. Chen, “Beamforming based on null-steering with small spacing linear microphone arrays,” *The Journal of the Acoustical Society of America*, vol. 143, no. 5, pp. 2651–2665, 2018.
- [11] R. Schmidt, “Multiple emitter location and signal parameter estimation,” *IEEE Transactions on Antennas and Propagation*, vol. 34, no. 3, pp. 276–280, 1986.
- [12] R. Roy and T. Kailath, “ESPRIT-estimation of signal parameters via rotational invariance techniques,” *IEEE Transactions on Acoustics, Speech, and Signal Processing*, vol. 37, no. 7, pp. 984–995, 1989.

- [13] N. T. N. Tho, S. Zhao, and D. L. Jones, "Robust DOA estimation of multiple speech sources," in *Proc. ICASSP*, 2014, pp. 2287–2291.
- [14] J. H. DiBiase, *A high-accuracy, low-latency technique for talker localization in reverberant environments using microphone arrays*, Ph.D. thesis, Brown University, Providence, R.I., 2000.
- [15] M. Omologo and P. Svaizer, "Use of the crosspower-spectrum phase in acoustic event location," *IEEE Transactions on Speech and Audio Processing*, vol. 5, no. 3, pp. 288–292, 1997.
- [16] C. Knapp and G. C. Carter, "The generalized correlation method for estimation of time delay," *IEEE Transactions on Acoustics, Speech, and Signal Processing*, vol. 24, no. 4, pp. 320–327, 1976.
- [17] S. Markovich-Golan and S. Gannot, "Performance analysis of the covariance subtraction method for relative transfer function estimation and comparison to the covariance whitening method," in *Proc. ICASSP*, 2015, pp. 544–548.
- [18] L. Drude, C. Boeddeker, J. Heymann, R. Haeb-Umbach, K. Kinoshita, M. Delcroix, and T. Nakatani, "Integrating neural network based beamforming and weighted prediction error dereverberation.," in *Proc. INTERSPEECH*, 2018, pp. 3043–3047.
- [19] J. Heymann, L. Drude, and R. Haeb-Umbach, "Neural network based spectral mask estimation for acoustic beamforming," in *Proc. ICASSP*, 2016, pp. 196–200.
- [20] L. Pfeifenberger, M. Zöhrer, and F. Pernkopf, "Deep complex-valued neural beamformers," in *Proc. ICASSP*, 2019, pp. 2902–2906.
- [21] C. H. Taal, R. C. Hendriks, R. Heusdens, and J. Jensen, "An algorithm for intelligibility prediction of time–frequency weighted noisy speech," *IEEE Transactions on Audio, Speech, and Language Processing*, vol. 19, no. 7, pp. 2125–2136, 2011.
- [22] A. N. S. Institute S3.5-1997, "Methods for calculation of the speech intelligibility index," *American National Standards Institute (ANSI)*, 1997.
- [23] R. E. Zezario, S.-W. Fu, C.-S. Fuh, Y. Tsao, and H.-M. Wang, "STOI-Net: A deep learning based non-intrusive speech intelligibility assessment model," in *Proc. APSIPA*, 2020, pp. 482–486.
- [24] D. B. Ward and R. C. Williamson, "Beamforming for a source located in the interior of a sensor array," in *Proc. ISSPA*, 1999, vol. 2, pp. 873–876.
- [25] Y. Luo and N. Mesgarani, "Conv-TasNet: Surpassing ideal time–frequency magnitude masking for speech separation," *IEEE/ACM Transactions on Audio, Speech, and Language Processing*, vol. 27, no. 8, pp. 1256–1266, 2019.
- [26] Y. Liu and D. Wang, "Divide and conquer: A deep CASA approach to talker-independent monaural speaker separation," *IEEE/ACM Transactions on Audio, Speech, and Language Processing*, vol. 27, no. 12, pp. 2092–2102, 2019.
- [27] X. Le, H. Chen, K. Chen, and J. Lu, "DPCRN: Dual-path convolution recurrent network for single channel speech enhancement," *arXiv preprint arXiv:2107.05429*, 2021.
- [28] S.-W. Fu, C. Yu, T.-A. Hsieh, P. Plantinga, M. Ravanelli, X. Lu, and Y. Tsao, "MetricGAN+: An improved version of MetricGAN for speech enhancement," *arXiv preprint arXiv:2104.03538*, 2021.
- [29] Y.-J. Lu, X. Chang, C. Li, W. Zhang, S. Cornell, Z. Ni, Y. Masuyama, B. Yan, R. Scheibler, Z.-Q. Wang, et al., "ESPnet-SE++: Speech enhancement for robust speech recognition, translation, and understanding," *arXiv preprint arXiv:2207.09514*, 2022.
- [30] O. L. Frost, "An algorithm for linearly constrained adaptive array processing," *Proceedings of the IEEE*, vol. 60, no. 8, pp. 926–935, 1972.
- [31] E. A. P. Habets, J. Benesty, I. Cohen, S. Gannot, and J. Dmochowski, "New insights into the MVDR beamformer in room acoustics," *IEEE Transactions on Audio, Speech, and Language Processing*, vol. 18, no. 1, pp. 158–170, 2009.
- [32] S.-W. Fu, Y. Tsao, H.-T. Hwang, and H.-M. Wang, "Quality-net: An end-to-end non-intrusive speech quality assessment model based on blstm," *arXiv preprint arXiv:1808.05344*, 2018.
- [33] W. Huang and J. Feng, "Differential beamforming for uniform circular array with directional microphones," in *Proc. INTERSPEECH*, 2020, pp. 71–75.
- [34] R. Scheibler, E. Bezzam, and I. Dokmanić, "Pyroomacoustics: A python package for audio room simulation and array processing algorithms," in *Proc. ICASSP*, 2018, pp. 351–355.
- [35] J. B. Allen and D. A. Berkley, "Image method for efficiently simulating small-room acoustics," *The Journal of the Acoustical Society of America*, vol. 65, no. 4, pp. 943–950, 1979.
- [36] D. B. Paul and J. Baker, "The design for the Wall Street Journal-based CSR corpus," in *Speech and Natural Language: Proceedings of a Workshop Held at Harriman, New York, February 23-26, 1992*, 1992, pp. 357–362.
- [37] P. C. Loizou, *Speech enhancement: theory and practice*, CRC press, 2007.
- [38] A. Varga and H. J. M. Steeneken, "Assessment for automatic speech recognition: II. NOISEX-92: A database and an experiment to study the effect of additive noise on speech recognition systems," *Speech Communication*, vol. 12, no. 3, pp. 247–251, 1993.
- [39] M.-W. Huang, "Development of Taiwan Mandarin hearing in noise test," M.S. thesis, Department of speech language pathology and audiology, National Taipei University of Nursing and Health science, 2005.
- [40] J. Thiemann, N. Ito, and E. Vincent, "The diverse environments multi-channel acoustic noise database (DEMAND): A database of multichannel environmental noise recordings," *Proceedings of Meetings on Acoustics*, vol. 19, no. 1, pp. 035081, 2013.
- [41] A. W. Rix, J. G. Beerends, M. P. Hollier, and A. P. Hekstra, "Perceptual evaluation of speech quality (PESQ)-a new method for speech quality assessment of telephone networks and codecs," in *Proc. ICASSP*, 2001, pp. 749–752.
- [42] M. Wang, C. Boeddeker, R. G. Dantas, and A. Seelan, "PESQ (perceptual evaluation of speech quality) wrapper for python users," May 2022.
- [43] R. E. Zezario, S.-W. Fu, F. Chen, C.-S. Fuh, H.-M. Wang, and Y. Tsao, "Deep learning-based non-intrusive multi-objective speech assessment model with cross-domain features," *IEEE/ACM Transactions on Audio, Speech, and Language Processing*, vol. 31, pp. 54–70, 2022.